$SrAlSi_4N_7:Eu^{2+}$ − A Nitridoalumosilicate Phosphor for Warm White Light (pc)LEDs with Edge-Sharing Tetrahedra

Cora Hecht,[†] Florian Stadler,[†] Peter J. Schmidt,[‡] Jörn Schmedt auf der Günne,[†] Verena Baumann,[†] and Wolfgang Schnick*,[†]

Department Chemie and Biochemie, Lehrstuhl für Anorganische Festkörperchemie, Ludwig-Maximilians-Universität München, Butenandtstrasse 5−13 (D), D-81377 München, Germany, and Philips Research Laboratories, Solid State Lighting, Weisshausstrasse 2, D-52066 Aachen, Germany

Received December 1, 2008. Revised Manuscript Received February 23, 2009

The new nitridoalumosilicate phosphor $SrAlSi_4N_7:Eu^{2+}$ has been synthesized under nitrogen atmosphere at temperatures up to 1630 °C in a radio-frequency furnace starting from Sr metal, α-Si_3N_4, AlN, and additional Eu metal. The crystal structure of the host compound $SrAlSi_4N_7$ has been solved and refined on the basis of single-crystal and powder X-ray diffraction data. In the solid, there is a network structure of corner-sharing SiN_4 tetrahedra incorporating infinite chains of all edge-sharing AlN_4 tetrahedra running along [001] ($SrAlSi_4N_7$: $Pna2_1$ (No. 33), $Z = 8$, $a = 11.742(2)$ Å, $b = 21.391(4)$ Å, $c = 4.966(1)$ Å, $V = 12.472(4)$ Å^3, 2739 reflections, 236 refined parameters, $R1 = 0.0366$). The Eu^{2+}-doped compound $SrAlSi_4N_7:Eu^{2+}$ shows typical broadband emission originating from dipole-allowed $4f^6(^7F_J)5d^1 \rightarrow 4f^7(^8S_{7/2})$ transitions in the orange-red spectral region ($\lambda_{max} = 632$ nm for 2% Eu doping level, 450 nm excitation) with a spectral width of FWHM = 2955 (± 75) cm^{-1} and a Stokes shift $\Delta S = 4823$ (± 100) cm^{-1}. The luminescence properties make the phosphor an attractive candidate material as red component in trichromatic warm white light LEDs with excellent color rendition properties.

Introduction

In 1993 Nakamura et al. described the successful use of InGaN as semiconductor material in blue-emitting LEDs.[1] Since then, good progress has been made in the development of efficient white-light LEDs. Having blue light now available originating from highly efficient LEDs, there are in general two methods to generate white light by additive color mixing. Besides joining three primary LEDs in red, green, and blue, most commonly, a blue primary LED is combined with a phosphor layer that partially converts the initial blue light into the complementary color, yielding white-light, phosphor-converted pc-LEDs. However, white light generated by adding only a single phosphor emitting in the orange-yellow spectral range (e.g., YAG:Ce)[2] is appropriate only if insufficient color rendering is acceptable. Furthermore, warm white light illumination usually cannot be achieved by this approach because of the lack of red spectral emission in such pc-LEDs.[3] Hence, for general illumination purposes in pc-LEDs, typically two phosphors, one yellow-green (e.g., $SrSi_2O_2N_2:Eu$)[4] and one orange-red (e.g., $Sr_2Si_5N_8:Eu$)[5] are employed in order to attune color rendering similar to blackbody radiation.[6] Eu^{2+}-doped host lattices turned out to be specifically suitable for this application.[6] The emitted wavelength of these phosphors depends on the host lattice of the rare-earth ion Eu^{2+}. The stronger (and more covalent) the ligand−activator bonding interactions and thus the crystal field strength afflicting the activator ions, the lower the energy difference between the $4f^6(^7F_J)5d^1$ and $4f^7(^8S_{7/2})$ states. This nephelauxetic effect leads to a red shift of the Eu^{2+} absorption and emission bands.[7,8]

The employed phosphors also need to be chemically and thermally quite stable in order to prevent degradation with heat and age, thus losing efficiency and causing changes in the produced light color. Condensed nitridosilicates doped with Eu^{2+} feature these preconditions, as well as excellent efficiency values with low thermal quenching, and have proved to be particularly suitable as luminescent materials, if excitable in the blue to near UV range of the spectrum.[6] Formally derived from classical oxosilicates by exchanging oxygen for nitrogen, the substance class of nitridosilicates allows for a richer structural diversity. Additionally to bridging only two tetrahedra like oxygen in classical (oxo)-silicates, nitrogen can also bridge three or even four neighboring tetrahedral centers, thus making a higher degree

* To whom correspondence should be addressed. E-mail: wolfgang.schnick@uni-muenchen.de.
† Ludwig-Maximilians-Universität München.
‡ Philips Research Laboratories.

(1) (a) Nakamura, S.; Fasol, G. *The Blue Laser Diode*; Springer: Berlin, 1997. (b) Nakamura, S *MRS Bull.* **1997**, *22*, 29.
(2) (a) Bando, K. *Proceedings of the 8th International Symposium on the Science and Technology of Light Sources*; Greifswald, Germany, Aug. 30−Sept. 3, 1998; Institute for Low-Temperature Plasma Physics: Greifswald, Germany, 1998; p 80. (b) Nakamura, S. *Proc. SPIE* **1997**, *3002*, 26. (c) Robbins, D. J. *J. Electrochem. Soc.* **1979**, *126*, 1550.
(3) Mueller-Mach, R.; Mueller, G. O. *Proc. SPIE* **2000**, *3938*, 30.
(4) Oeckler, O.; Stadler, F.; Rosenthal, T.; Schnick, W. *Solid State Sci.* **2007**, *9*, 205.
(5) Schlieper, T.; Milius, W.; Schnick, W. *Z. Anorg. Allg. Chem.* **1995**, *621*, 1380.
(6) Mueller-Mach, R.; Mueller, G.; Krames, M. R.; Höeppe, H. A.; Stadler, F.; Schnick, W.; Juestel, T.; Schmidt, P. *Phys. Status Solidi A* **2005**, *202*, 1727.
(7) Dorenbos, P. *Phys. Rev. B* **2002**, *65*, 235110/1.
(8) Shi, J. S.; Zhang, S. Y. *J. Phys. Chem. B* **2004**, *108*, 18845.

10.1021/cm803231h CCC: $40.75
Published on Web 03/24/2009

of condensation possible.[9] Furthermore, because of the higher polarizability of nitrogen, interconnection of SiN_4 tetrahedra via common edges was frequently observed in nitridosilicates. For example, the structures of $MSiN_2$ (M = Ba, Sr),[10] MSi_7N_{10} (M = Ba, Sr),[11,12] and $Ba_5Si_2N_6$[13] feature edge-sharing SiN_4 tetrahedra.

Besides oxosilicates, nitridosilicates, and oxonitridosilicates,[14] there is an extension that further augments the structural diversity in silicate chemistry. Partial formal substitution of silicon by aluminum leads to nitridoalumosilicates, which are scarcely investigated so far. Up to date, no mineral has been detected in this class and the only known synthetic examples are $MSiAlN_3$ (M = Be, Mg, Mn, Ca),[15] $Ca_5Si_2Al_2N_8$,[16] $Ca_4SiAl_3N_7$,[17] $La_{17}Si_9Al_4N_{33}$,[18] filled α-Si_3N_4-type compounds,[19] and $Ba_2Si_5AlN_9$.[20]

In this contribution, we report about the synthesis, crystal structure, and luminescence properties of the new nitridoalumosilicate $SrAlSi_4N_7$, which represents a new type of nitridoalumosilicate featuring infinite chains of edge-sharing AlN_4 tetrahedra. Additionally, the interesting luminescence properties have been investigated, showing possible application in warm, white-light-emitting pc-LEDs.

Experimental Section

Synthesis and Chemical Analysis. The host compound $SrAlSi_4N_7$ was prepared by high-temperature synthesis in a radio-frequency furnace[21] starting from 1.0 mmol (41.0 mg) AlN (Tokuyama, Tokyo, 99.9%), 0.67 mmol (93.5 mg) α-Si_3N_4 (Ube Industries Ltd., Tokyo, 98%), and 0.5 mmol (43.8 mg) Sr (ABCR GmbH & Co. KG, Karlsruhe, 99.95%). The starting materials were mixed in an agate mortar and filled into a tungsten crucible under argon atmosphere in a glovebox (Unilab, MBraun; $O_2 < 1$ ppm, $H_2O < 1$ ppm). For the synthesis of $SrAlSi_4N_7$:Eu^{2+} 2% of the Sr metal was substituted for Eu, using EuF_3 as dopant (Aldrich Chemical Co., Milwaukee, 99.99% (metal basis)), but other doping agents (e.g., $EuCl_2$, Eu metal) work as well.

The crucible was placed into the center of the induction coil of the radio-frequency generator inside the water cooled silica glass reactor under purified N_2 atmosphere. The reaction mixture was heated to 1630 °C within 3 h. After an annealing time of 5 h at this temperature, the crucible was cooled to 1230 °C in another 5 h, and then quenched to room temperature by switching off the furnace. $SrAlSi_4N_7$ was obtained as a well crystalline product, either colorless or orange if doped with 2% Eu, respectively. Usually, microcrystalline $Sr_2Si_5N_8$ appeared as byproduct, especially when the starting materials have been mixed stoichiometrically. However, the impurities could be separated and removed by flotation with isopropyl alcohol.

Table 1. Crystallographic Data and Structure Refinement of $SrAlSi_4N_7$

formula	$SrAlSi_4N_7$
mol wt (g mol^{-1})	325.03
cryst syst	orthorhombic
space group	$Pna2_1$ (No. 33)
T (K)	293
diffractometer	STOE IPDS
radiation, λ (Å)	Mo-K_α, 0.71073
a (Å)	11.742(2)
b (Å)	21.391(4)
c (Å)	4.966(1)
V (Å^3)	1247.2(4)
Z	8
ρ_{calcd} (g cm^{-3})	1.731
$F(000)$	624
μ (mm^{-1})	4.749
cryst size (mm^3)	0.10 × 0.07 × 0.05
diffraction range	$3.34 \le \theta \le 30.00$
index range	$-17 \le h \le 17$, $-32 \le k \le 30$, $-6 \le l \le 6$
total no of reflns	12701
independent reflns	3329
obsd reflns	2739 ($R_{int} = 0.0370$)
refined params	236
corrections	absorption, Lorentz, polarization
absorp corr	numerical
min./max. transmission ratio	0.4579/0.6728
min./max. residual electron density (e Å^{-3})	−0.989/0.662
GOF	0.993
final R indices [$I > 2\sigma(I)$]	$R1 = 0.0366$, $wR2 = 0.0873$
R indices (all data)	$R1 = 0.0477$, $wR2 = 0.0913$[a]

[a] $w = [\sigma^2(F_o^2) + (0.0000\ P)^2 + 0.4464\ P]^{-1}$, where $P = (F_o^2 + 2F_c^2)/3$.

Semiquantitative elemental analyses were performed on a JSM-6500F scanning electron microscope (Jeol) by energy-dispersive X-ray spectroscopy (EDX) with a Si/Li EDX detector (Oxford Instruments, model 7418). In accordance to the structure model, the composition is within the typical error ranges (Calcd for $SrAlSi_4N_7$: Sr, 27; Al, 8; Si, 35; N, 30 wt %. Found: Sr, 27; Al, 8; Si, 33; N, 32 wt %). More precise results have been obtained from a Eu-doped sample (double determination, Mikroanalytisches Labor Pascher, Remagen, Germany). Calcd for $Sr_{0.98}AlSi_4N_7$:$Eu_{0.02}$: Sr, 26.3; Al, 8.3; Si, 34.4; N, 30.0; Eu, 0.9. Found: Sr, 25.1; Al, 9.15; Si, 33.3; N, 27.8; O, 1.5; Eu, 1.0 wt %). However, these investigations were indicative of small amounts of oxygen, probably originating from slightly contaminated Si_3N_4 or Sr. Apparently, small amounts of oxygen are quite inevitable in nitridoalumosilicates.[16,17] However, the charge balance in these compounds can easily be achieved by slightly adjusting the molar ratio Si:Al.

Single-Crystal X-ray Analysis. Single-crystal X-ray diffraction data was collected on a STOE IPDS I diffractometer (Stoe & Cie., Darmstadt, Germany) with Mo Kα radiation (0.71073 Å, graphite monochromator). The structure was solved by direct methods and refined in space group $Pna2_1$, using the SHELX suite of programs for all calculations.[22,23] All atoms have been refined anisotropically. Details regarding the data collection and refinement are summarized in Table 1. Atomic coordinates, displacement parameters, and site occupancy factors are given in the Supporting Information. Further details of the structure determination and refinement are available

(9) Schnick, W.; Huppertz, H. *Chem.—Eur. J.* **1997**, *3*, 679.
(10) Gál, Z. A.; Mallinson, P. M.; Orchard, H. J.; Clarke, S. J. *Inorg. Chem.* **2004**, *43*, 3998.
(11) Huppertz, H.; Schnick, W. *Chem.—Eur. J.* **1997**, *3*, 249.
(12) Pilet, G.; Hoeppe, H. A.; Schnick, W.; Esmaeilzadeh, S. *Solid State Sci.* **2005**, *7*, 391.
(13) Yamane, H.; DiSalvo, F. J. *J. Alloys Compd.* **1996**, *240*, 33.
(14) Schnick, W. *Int. J. Inorg. Mater* **2001**, *3*, 1267.
(15) Thompson, D. P. *Mater. Sci. Forum* **1989**, *47*, 21.
(16) Ottinger, F. Ph.D. Thesis (Diss. ETH Nr. 15624), ETH Zürich, Zürich, Switzerland, 2004.
(17) Ottinger, F.; Kroslakova, I.; Hametner, K.; Reusser, E.; Nesper, R.; Guenther, D. *Anal. Bioanal. Chem.* **2005**, *383*, 489.
(18) Pilet, G.; Grins, J.; Edèn, M.; Esmaeilzadeh, S. *Eur. J. Inorg. Chem.* **2006**, *18*, 3627.
(19) Grins, J.; Esmaeilzadeh, S.; Shen, Z. *J. Am. Ceram. Soc.* **2003**, *86*, 727.
(20) Kechele, J. A.; Hecht, C.; Oeckler, O. , Schmedt auf der Günne, J.; Schmidt, P. J.; Schnick, W. *Chem. Mater.* **2009**, *21*, DOI: 10.1021/cm803233d.
(21) Schnick, W.; Huppertz, H.; Lauterbach, R. *J. Mater. Chem.* **1999**, *9*, 289.
(22) Sheldrick, G. M. *Acta Crystallogr., Sect. A* **2008**, *64*, 112.
(23) Farrugia, L. J. *J. Appl. Crystallogr.* **1999**, *32*, 837.

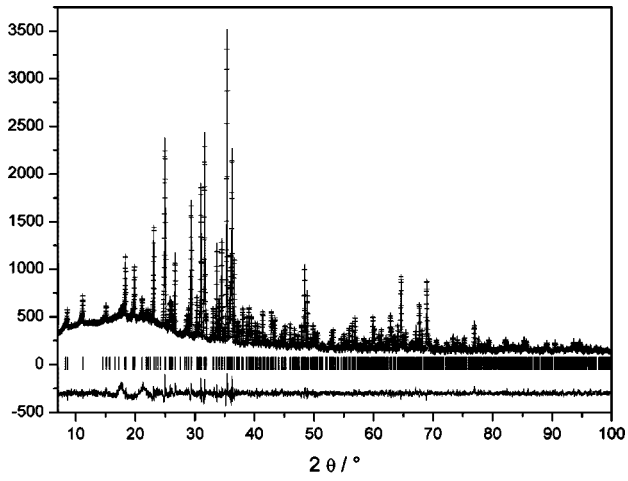

Figure 1. Rietveld refinement plot for $SrAlSi_4N_7$. Observed (crosses), calculated (line), and difference profile of the X-ray powder diffraction are plotted on the same scale. Bragg peaks are indicated by vertical bars.

Table 2. Details of the Rietveld Refinement of $Sr_{0.98}AlSi_4N_7:Eu_{0.02}$

formula	$Sr_{0.98}AlSi_4N_7:Eu_{0.02}$
mol wt (g mol^{-1})	326.28
cryst syst	orthorhombic
space group	$Pna2_1$ (No. 33)
radiation, λ (Å)	Cu-K_α, 1.54056
a (Å)	11.7046(2)
b (Å)	21.3148(3)
c (Å)	4.9503(1)
V (Å^3)	1235.01(4)
Z	8
ρ_{calcd} (g cm^{-3})	1.755
profile range	$5.5 \leq 2\theta \leq 100$
no. of data points	9451
positional params	127
profile params	19
R values	$R_F^2 = 0.06547$, wR_P (fit) = 0.0664, R_P (fit) = 0.0523, wR_P (back) = 0.0628, R_P (back) = 0.0530

from Fachinformationszentrum Karlsruhe, 76344 Eggenstein-Leopoldshafen, Germany (fax (49)7247−808−666; e-mail crysdata@fiz-karlsruhe.de; http://www.fiz-karlsruhe.de/request_for_deposited_data.html) on quoting the deposition number CSD-380271.

X-ray Powder Diffraction. X-ray powder diffraction patterns were recorded in Guinier geometry using a Huber G670 imaging plate detector (Cu $K\alpha_1$ radiation, Ge(111) monochromator). Rietveld refinement was performed with the GSAS program package[24] starting from the structure parameters obtained from the single-crystal X-ray refinement. Table 2 shows the crystallographic data and details. A plot of the Rietveld refinement with the observed and calculated patterns, including the corresponding difference profile is given in Figure 1.

Photoluminescence Measurements. Excitation (PLE), emission (PL), and reflection spectra were recorded with an intregrated setup based on a fiber spectrometer (Avantes 2000, 75 W xenon lamp) and an integrating sphere (Labsphere). To determine the spectral response function of the detection system, we have used a calibration halogen lamp and different standard inorganic broadband emitting phosphors (spectral power distribution determined by the Physikalische Technische Bundesanstalt, Berlin, Germany). Luminescence quantum efficiencies were determined by comparing absorption and emission data with standard phosphors ($Sr_2Si_5N_8$:Eu, 86% QE for 450 nm excitation; YAG:Ce, U728, Philips Lighting, 90% QE for 450 nm excitation).

Solid-State NMR Measurements. The NMR experiments were carried out on a BRUKER Avance DSX 500 spectrometer equipped with a commercial 4 mm MAS NMR probe. The magnetic field strength was 11.75 T corresponding to ^{29}Si and ^{27}Al resonance frequencies of 99.5 and 130.5 MHz, respectively. The deshielding values reported for ^{29}Si and ^{27}Al refer to 1% $Si(CH_3)_4$ in $CDCl_3$ and a solution of $Al(NO_3)$ 1.1 mol kg^{-1} in D_2O. The ^1H resonance of 1% $Si(CH_3)_4$ in $CDCl_3$ served as an external secondary reference using the Ξ values for ^{29}Si and ^{27}Al as reported by the IUPAC.[25] Saturation combs were applied prior to all repetition delays. The ^{29}Si spectrum was acquired on a Eu doped sample with a repetition delay of 64 s at a sample spinning frequency of 9 kHz. A triple-quantum ^{27}Al MQMAS 2D spectrum was acquired on a non doped sample using a three-pulse sequence with a zero-quantum filter,[26] a repetition delay of 64 s,and rotor-synchronized sampling of the indirect dimension. Phase cycling involved the States method for acquisition of pure absorption line shapes and a 48 step phase cycle for coherence transfer pathway selection. Chemical shift values were determined by moment analysis[27] from the extracted rows of the sheared MQMAS spectrum.

Neutron Powder Diffraction. Time-of-flight (TOF) neutron powder diffraction measurements have been carried out at the GEM diffractometer at ISIS (Rutherford Appleton Laboratory, Chilton, U.K.), which is well suited for the measurement of small amounts of sample. The experiment has been conducted at room temperature on a sample of $Sr_{0.98}AlSi_4N_7:Eu_{0.02}$ (about 250 mg) that has been enclosed in a vanadium can (diameter 6 mm). For the evaluation of the neutron diffraction data, the GSAS program package[24] was employed.

Results and Discussion

Crystal Structure. The nitridoalumosilicate host compound $SrAlSi_4N_7$ contains a highly condensed network structure build-up on SiN_4 and AlN_4 tetrahedra. Although the stoichiometric formula may suggest a similarity to the already well-known compounds $MYbSi_4N_7$ (M = Sr, Ba)[28] and isotypic $MYSi_4N_7$ (M = Sr, Ba),[29] $SrAlSi_4N_7$ shows no structural resemblance to them at all. For example, it does not contain star-shaped building blocks with N^4-type nitrogen atoms. Moreover, in $SrAlSi_4N_7$, the tetrahedra are not only linked via common corners but the structure also contains infinite chains of all edge-sharing tetrahedra running along [001], which are presumably centered by aluminum. These *trans*-linked chains are connected through common corners with the nitridosilicate network (Figures 2 and 3), pervaded with channels alongside the chains. The channels host two different Sr^{2+} positions that are coordinated by irregular polyhedra made-up of six or eight nitrogen atoms, respectively (Figure 4). The distances Sr−N range between 250.4(5) and 314.3(5) pm for Sr1 and between 265.3(7) and 305.7(6) pm for Sr2 (for details see Supporting Information). The N^2 atoms coordinate two Sr^{2+} while the N^3 atoms are

(24) Larson, A. C.; Von Dreele, R. B. , *GSAS−General Structure Analysis System*; Report LAUR 86-748; Los Alamos National Laboratory: Los Alamos, NM, 1998.

(25) Harris, R. K.; Becker, E. D.; Cabral de Menezes, S. M.; Granger, P.; Hoffman, R. E.; Zilm, K. W. *Pure Appl. Chem.* **2008**, *80*, 59.

(26) Amoureux, J.-P.; Fernandez, C.; Steuernagel, S. *J. Magn. Reson.* **1996**, *A123*, 116.

(27) Herreros, B.; Metz, A. W.; Harbison, G. S. *Solid State Nucl. Magn. Reson.* **2000**, *16*, 141.

(28) Huppertz, H.; Schnick, W. Z. *Anorg. Allg. Chem.* **1997**, *623*, 212.

(29) Fang, C. M.; Li, Y. Q.; Hintzen, H. T.; de With, G. *J. Mater. Chem.* **2003**, *13*, 1480.

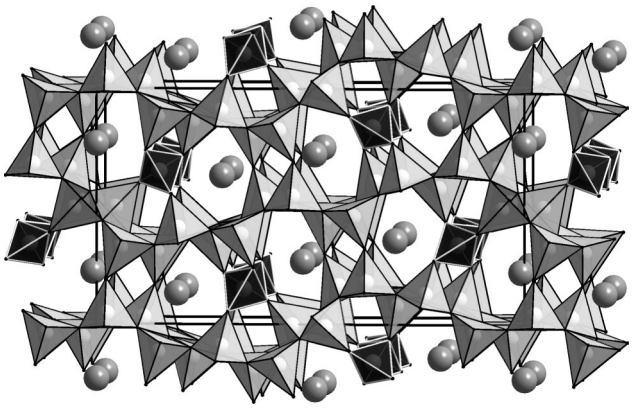

Figure 2. Structure of $SrAlSi_4N_7$ (view along [001]). The chains of edge-sharing tetrahedra are marked in dark gray.

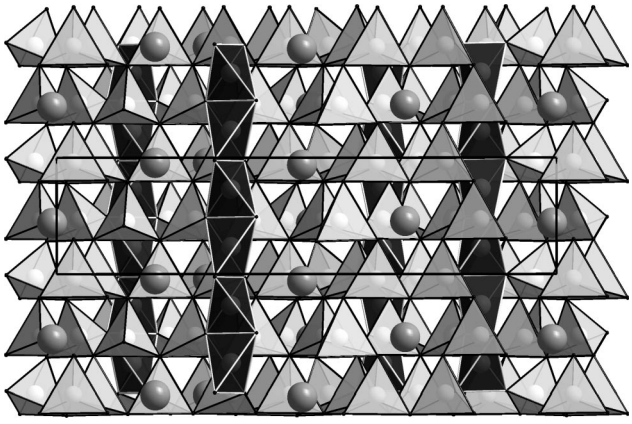

Figure 3. Crystal structure of $SrAlSi_4N_7$ (view along [100]). The chains of edge-sharing tetrahedra are marked in dark gray.

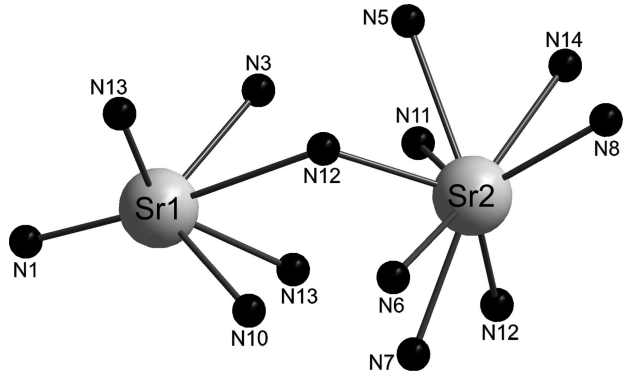

Figure 4. Coordination spheres of the two different Sr^{2+} positions in $SrAlSi_4N_7$.

only neighboring one Sr^{2+}. The bond lengths of the bridging N^2 to the tetrahedral centers are within 168.5(6) to 173.6(5) pm, whereas the distances for N^3 are slightly longer (172.9(5) and 182.1(6) pm). Within the chains of edge-sharing tetrahedra the distances between the tetrahedral centers and the nitrogen atoms are quite similar, ranging from 173.1(7) to 182.0(8) pm. All values are in the typical range for Si−N or Al−N bonds ($Sr_2Si_5N_8$:[5] 165.3−1.786 pm; $SrSi_7N_{10}$:[12] 165.9−180.1 pm; $CaAlSiN_3$:[15] 179.0 pm; $Sr_3Al_2N_4$:[30] 188.5−195.8 pm). Specifically interesting is the geometric

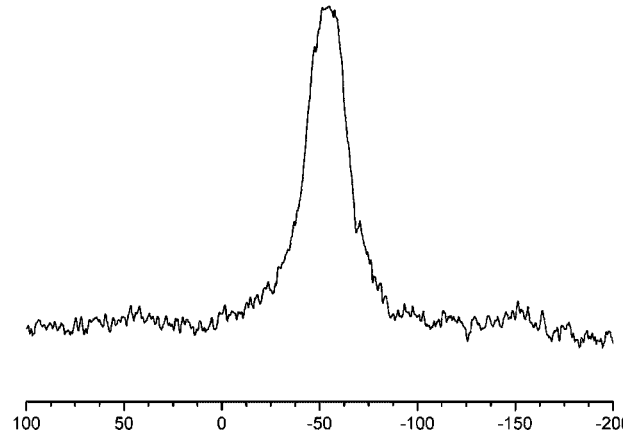

Figure 5. ^{29}Si solid-state NMR of $SrAlSi_4N_7$:Eu with a broad signal at −55 ppm; T_1 values of nondoped $SrAlSi_4N_7$ are so long that no intensity was observed in 24 h experimental time.

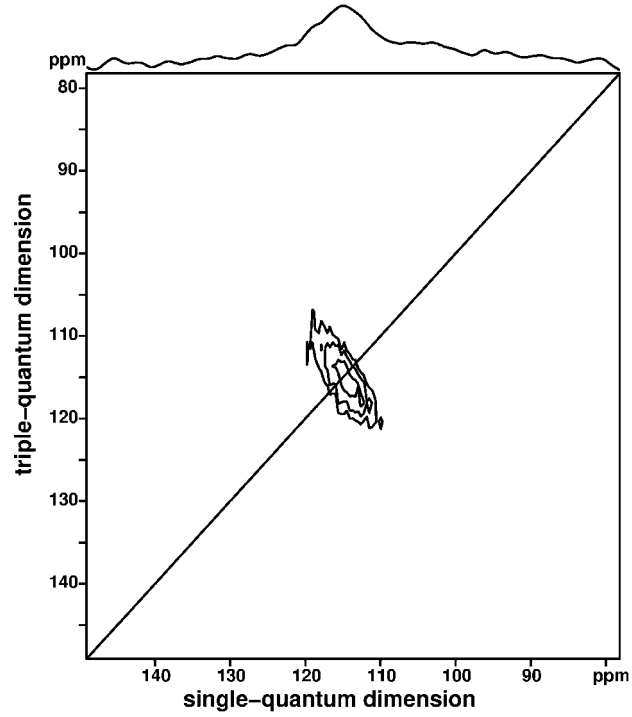

Figure 6. ^{27}Al MQ-MAS NMR. A broad signal at 114.5 ppm is observed in the typical range for AlN_4 tetrahedra.

situation inside these chains (Figure 5), which are almost linear. The four angles enclosed by the Al_2N_2 units are adding up to values of 359.9 and 359.6°, respectively. The included angle between the aluminum tetrahedra centers amounts 179.2(2)°, thus deviating only slightly from 180°. For all other Q^4-type tetrahedra, which are presumably centered by Si^{4+}, the tetrahedral angles are in the normal range between 104.6(3)° and 114.3(3)°.

The complex structure of $SrAlSi_4N_7$ contains 10 different Si/Al sites, each on Wyckoff positions 4*a*. The results of the chemical and structural analyses suggest that two out of these ten positions should be exclusively occupied by Al, confirming the empirical formula $SrAlSi_4N_7$, which was previously established by charge balancing arguments. Unlike Si^{4+}, aluminum (Al^{3+}) seems to be predestined being situated on the tetrahedral centers of the infinite chains made up of edge-sharing tetrahedral TN_4. The distance between two

(30) Ludwig, M.; Niewa, R.; Kniep, R. *Z. Naturforsch., B: Chem. Sci.* **1999**, *54*, 461.

Table 3. MAPLE Values for $SrAlSi_4N_7$, Assuming an Ordered Si/Al Distribution Where Al^{3+} Occupies Exclusively the Edge-Sharing Tetrahedra (all values in kJ mol^{-1})[a]

Partial MAPLE Values for $SrAlSi_4N_7$					
$Sr(1)^{2+}$	1752	$Si(8)^{4+}$	9240	$N(7)^{3-}$	6012
$Sr(2)^{2+}$	1766	$Al(1)^{3+}$	6215	$N(8)^{3-}$	5133
$Si(1)^{4+}$	9714	$Al(2)^{3+}$	6461	$N(9)^{3-}$	5761
$Si(2)^{4+}$	9776	$N(1)^{3-}$	5301	$N(10)^{3-}$	5991
$Si(3)^{4+}$	9002	$N(2)^{3-}$	5085	$N(11)^{3-}$	6199
$Si(4)^{4+}$	9939	$N(3)^{3-}$	6226	$N(12)^{3-}$	5530
$Si(5)^{4+}$	9600	$N(4)^{3-}$	5053	$N(13)^{3-}$	5573
$Si(6)^{4+}$	9350	$N(5)^{3-}$	6050	$N(14)^{3-}$	5951
$Si(7)^{4+}$	9320	$N(6)^{3-}$	5890		

Partial MAPLE Values for Comparison	
Sr^{2+}	1805 − 2108 (in $SrSiO_3$);[34] 1790 − 1832 (in $Sr_3Al_2N_4$)[30]
Si^{4+}	9316/9349 (in $Ba_3Si_6O_9N_4$);[35] 9555/9875 (in $BaSi_6N_8O$)[36]
Al^{3+}	5434 (in AlN);[37] 5434/5521 (in $Ba_3Al_2N_4$)[30]
N^{3-}	5938/5999 (in Si_3N_4);[38] 6143 (in Si_2N_2O);[39] 5236 − 6150 (in $Sr_2Si_5N_8$)[5]

[a] Coulomb part of lattice energy for $SrAlSi_4N_7$: 85939. Theoretical Coulomb part of lattice energy: 86416, (according to 1/2 $Sr_2Si_5N_8$ + 1/2 α-Si_3N_4 + AlN = $SrAlSi_4N_7$; with $Sr_2Si_5N_8$ = 98133, α-Si_3N_4 = 53017; AlN = 10841).

adjacent tetrahedra centers is shorter in case of edge-sharing, accordingly the less charged cations (Al^{3+}) could be electrostatically favored on these sites. MAPLE (Madelung Part of Lattice Energy) calculations [31−33] suggest an ordered distribution of Si and Al, but can not determine whether Al^{3+} is exclusively positioned inside the edge-sharing tetrahedra chains. Table 3 gives the results of a MAPLE calculation with an ordered Si/Al distribution. For this calculation Al^{3+} was placed exclusively on the positions forming the edge-sharing tetrahedra chains, which means all only corner-sharing tetrahedra are occupied by Si^{4+}. Compared to a theoretical calculated value for the expected Coulomb part of lattice energy (according to 1/2 $Sr_2Si_5N_8$ + 1/2 α-Si_3N_4 + AlN = $SrAlSi_4N_7$), the obtained value for $SrAlSi_4N_7$ deviates 0.55% when assuming this model. If for the calculation a complete Si/Al disorder was taken as a basis, the discrepancy added up to 0.99%. Table 3 also shows the partial MAPLE values for the above-mentioned ordered structure model as well as several values of structural reliable compounds for comparison. For Sr^{2+}, Si^{4+}, and N^{3-}, the partial MAPLE values are well within the expected range. For Al^{3+} usually partial MAPLE values about 5500 kJ mol^{-1} are observed. However, all our calculations with any ordered Si/Al distribution showed partial MAPLE values of Al^{3+} above 6000 kJ mol^{-1}. Because Si^{4+} in nitridosilicates and oxonitridosilicates usually has values around 9500 kJ mol^{-1}, Al^{3+} seems to be predominantly localized at the centers of the edge-sharing tetrahedra; however, most likely the Si/Al distribution is subject to a certain extent of disorder. Similar disorder phenomena have already been investigated by first-principles pseudopotential methods for $CaAlSiN_3$,[40] the latter being an important host lattice for the respective Eu-doped red-light emitting phosphor materials. Gathering experimental evidence about a possible Si/Al order or disorder, however, is difficult. Neutron diffraction experiments can sometimes provide information, yet in this case the received data did not allow drawing any conclusions. The difference in the simulated diffraction patterns between possible Si/Al distributions proved to be too small compared to the signal-to-noise ratio of the experiment. An other experimental method that could yield answers to this question is solid-state NMR. Having an influence on the close proximity of a tetrahedra center, the connection type should also affect the ^{29}Si and ^{27}Al signals in the solid-state NMR experiment. If one of the two crystallographic positions within the chains is occupied by Al^{3+} together with any of the other positions that are connected only via common corners, than the ^{27}Al and ^{29}Si signals should both split into two signals. However, only one signal is discernible in either experiment (Figures 5 (doped sample) and 6 (undoped sample)). The ^{29}Si-experiment could only be conducted on a doped sample, because the T_1-values of the nondoped $SrAlSi_4N_7$ are so long, that no intensity was observed in 24 h experimental time. This results in a broad ^{29}Si-signal that could not be resolved into the respective individual signals. The ^{27}Al MQMAS measurement on the undoped sample also showed only one peak, which is narrower, but still quite broad. This suggests, that either alumina is indeed only located within the chains, or that the case of two superimposed signals occurs. Lacking comparative data in literature for edge-sharing tetrahedra in nitridoalumosilicates, no definite conclusion can be drawn at this time. We hope that the progress in the research of nitridoalumosilicates allows an exact distinction in the near future.

Yet, there are only a very few other silicate structures in the literature containing edge-sharing tetrahedra chains. The sole Si−O compound dates back to 1954, when Weiss et al. described a 'fibrous' silicon dioxide modification, supposedly made up exclusively of linear chains, parallel-running and unlinked.[41] However, this modification remains irreproducible and controversial. On the other hand, the structure of $M_3Al_2N_4$ (M = Sr, Ba),[30,42] is already well confirmed. It consists of parallel-running chains of edge-sharing AlN_4 tetrahedra, but in this case the chains are comparably curved and coordinate Sr^{2+} in between.

Luminescence. Eu^{2+}-doped $SrAlSi_4N_7$ powder samples were obtained by using EuF_3 as dopant. The bright orange-red body color of the samples is similar to $M_2Si_5N_8$:Eu (M

(31) Hoppe, R. , Angew. Chem. 1966, *78*, 52, Angew. Chem. Int. Ed., 1966, 5, 95.
(32) Hoppe, R. *Angew. Chem.* **1970**, *82*, 7; *Angew. Chem., Int. Ed.* **1970**, *9*, 25.
(33) Hübenthal, R. MAPLE, Programm zur Berechnung des Madelunganteils der Gitterenergie, version 4; Universität Giessen: Giessen, Germany, 1993.
(34) Machida, K. I.; Adachi, G. Y.; Shiokawa, J.; Shimada, M.; Koizumi, M. *Acta Crystallogr., Sect. B* **1982**, *24*, 1968.
(35) Stadler, F.; Schnick, W. *Z. Anorg. Allg. Chem.* **2006**, *632*, 949.
(36) Stadler, F.; Kraut, R.; Oeckler, O.; Schmid, S.; Schnick, W. *Z. Anorg. Allg. Chem.* **2005**, *631*, 1773.
(37) Christensen, N. E.; Gorczyca, I. *Phys. Rev. B: Condens. Matter* **1994**, *50*, 4397.
(38) Yang, P.; Fun, H.-K.; Rahman, I. A.; Saleh, M. I. *Ceram. Int.* **1995**, *21*, 137.
(39) Sjoeberg, J.; Helgesson, G.; Idrestedt, I. *Acta Crystallogr., Sect. C* **1991**, *47*, 2438.
(40) Mikami, M.; Uheda, K.; Kijima, N. *Phys. Status Solidi A* **2006**, *203*, 2705.
(41) Weiss, A.; Weiss, A. *Z. Anorg. Allg.* **1954**, *276*, 95.
(42) Blase, W.; Cordier, G.; Ludwig, M.; Kniep, R. *Z. Naturforsch., B: Chem. Sci.* **1994**, *49*, 501.

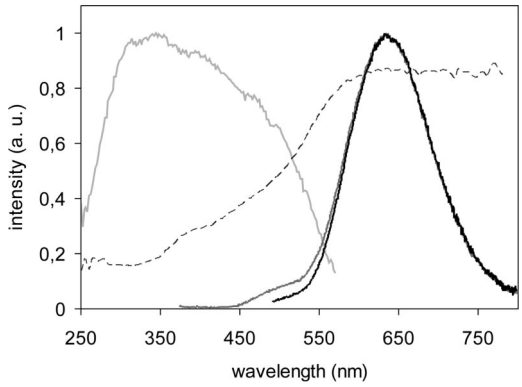

Figure 7. Room-temperature emission spectrum for 450 and 350 nm excitation (black and dark gray curves, respectively), excitation spectrum monitored at 635 nm (light gray curve) and reflection spectrum (dashed line) of $Sr_{0.98}AlSi_4N_7:Eu_{0.02}$.

= Sr, Ba) type phosphors[5,43,44] indicating strong broadband absorption in the blue to green spectral range by Eu activators in the divalent state, situated on both Sr sites.

Figure 7 shows excitation, emission, and reflection spectra for a $Sr_{0.98}AlSi_4N_7:Eu_{0.02}$ sample. The reflectance spectrum shows broad absorption bands in the UV to green spectral region with a similar shape as known from $M_2Si_5N_8$:Eu (M = Sr, Ba) type phosphors. [5,43,44] For blue excitation, a broadband spectrum peaking at 635 nm is obtained showing a spectral width of FWHM = 2955 (±75) cm^{-1} and a Gaussian shape on a energy scale as expected for a large Stokes shift emission band from a single site. [45] By applying the mirror-image relationship between broad emission and absorption bands,[46] the zero-phonon energy E_0 can be estimated to be at ~566 nm. Values for Stokes shift and the lowest lying absorption band position are thus $\Delta S = 4823$ (± 100) cm^{-1} and ~494 nm, respectively.

Excitation of $SrAlSi_4N_7$:Eu at 350 nm (maximum of the excitation band in Figure 7) leads to a composed emission band that shows a shoulder at ~500 nm besides the red emission band, with the latter being identical with the band observed for 450 nm excitation (black curve in Figure 7). The occurrence of a composed emission band may be explained by Eu^{2+} emission from the two different Sr lattice sites. Since the coordination number and geometry differ significantly for Sr1 (CN = 6, $Sr-N_{avg}$ = 2.71 Å, shortest contact = 2.50 Å) and Sr2 (CN = 8, $Sr-N_{avg}$ = 2.87 Å, shortest contact = 2.65 Å) it can be expected that the 635 nm (500 nm) emission originates from Eu^{2+} located at Sr1 (Sr2) position, because the former position should show a larger crystal field strength (smaller CN) and shorter and thus more covalent activator−ligand contacts. These assumptions are supported by EHTB-MO calculations of the net positive charge of Eu located at the two different substitutional sites

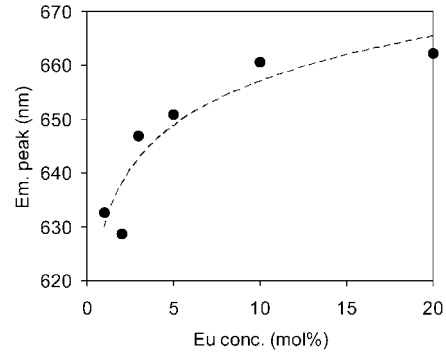

Figure 8. Peak intensity wavelength λ_{max} of the red emission of $SrAlSi_4N_7$:Eu as a function of the Eu concentration (λ_{exc} = 450 nm).

indicating significantly different charge populations.[47,48] Because the emission band of the short wavelength emitting center and the absorption band of the long wavelength center are overlapping energetically, the emission band at ~500 nm is only visible as a shoulder. A similar situation is known, for example, for $Sr_{1.95}Ba_{0.05}SiO_4$:Eu, where two emission bands from the two different cation sites can be observed at 495 and 570 nm if excited at 320 nm and only one broad emission band if excited at >400 nm because of a strong reabsorption.[49]

The dominating red emission band can be shifted toward larger wavelengths (630 − 660 nm) by increasing the Eu^{2+} concentration as depicted in Figure 8. In this doping range, the quantum efficiency decreases from 69 ± 2% to 55 ± 2% with increasing Eu^{2+} content as a consequence of concentration quenching. The absorption and emission properties of $SrAlSi_4N_7$:Eu make this material an attractive candidate material for use in white, phosphor-converted LEDs. For example, the combination of a green-emitting phosphor like $SrSi_2O_2N_2$:Eu and red-emitting $SrAlSi_4N_7$:Eu can be used to build trichromatic, warm white LEDs (correlated color temperature ~3200 K) based on 450 nm pump LEDs that show excellent color rendering properties (R_a8: 86−93).

Conclusions

The promising new nitridoalumosilicate phosphor $SrAlSi_4N_7$:Eu has been obtained by reacting Sr, Si_3N_4, AlN, and an Eu-dopant at 1630 °C in a radio-frequency furnace. The determined structure of the framework is remarkable, showing infinite parallel-running one-dimensional chains of edge-sharing tetrahedra that are presumably centered solely by alumina. The Eu-doped compound features excellent luminescence properties with a broadband emission spectrum peaking at 632 nm, thus having the potential to be employed in phosphor converted warm-white-light-emitting diodes (pc-LEDs).

Acknowledgment. The authors thank Christian Minke (Department of Chemistry & Biochemistry, LMU München) for

(43) Höppe, H. A.; Lutz, H.; Morys, P.; Schnick, W.; Seilmeier, A. *J. Phys. Chem. Solids* **2000**, *61*, 2001.
(44) Li, Y. Q.; van Steen, J. E. J.; van Krevel, J. W. H.; Botty, G.; Delsing, A. C. A.; DiSalvo, F. J.; deWith, G.; Hintzen, H. T. *J. Alloys Compd.* **2006**, *417*, 273.
(45) Henderson, B.; Imbush, G. F. *Optical Spectroscopy of Inorganic Solids*; Clarendon Press: Oxford, 1989.
(46) Nazarov, M.; Tsukerblat, B.; Noh, D. Y. *J. Phys. Chem. Solids* **2008**, *69*, 2605.
(47) Gauthier, G.; Jobic, S.; Evain, M.; Koo, H.-J.; Whangbo, M.-H.; Fouassier, C.; Brec, R. *Chem. Mater.* **2003**, *15*, 828.
(48) Schmidt, P.; Tuecks, A.; Meyer, J.; Bechtel, H.; Wiechert, D.; Mueller-Mach, R.; Mueller, G.; Schnick, W. *Proc. SPIE* **2008**, *6669*, 66690P–1.
(49) Poort, S. H. M. Ph.D. Thesis, Utrecht University, Utrecht, The Netherlands, 1997.

solid-state NMR measurements and for conducting the EDX and REM measurements and Thomas Miller (Department of Chemistry & Biochemistry, LMU München) for collecting the single-crystal X-ray diffraction data. Financial support by the Fonds der Chemischen Industrie (FCI), Germany, is gratefully acknowledged.

Supporting Information Available: Tables of atomic coordinates and anisotropic displacement parameters for $SrAlSi_4N_7$, as well as bond length for Sr−N and Al−N (PDF). This material is available free of charge via the Internet at http://pubs.acs.org.

CM803231H